Short-length carbon nanotubes as building blocks for high dielectric constant materials in the terahertz range

Mikhail Shuba, Alesia Paddubskaya, Polina Kuzhir, Sergey Maksimenko, Emmanuel Flahaut, Vanessa Fierro, Alain Celzard, Gintaras Valušis

doi:10.1088/1361-6463/aa5628

Short-length carbon nanotubes as building blocks for high dielectric constant materials in the terahertz range

M V Shuba[1,7], A G Paddubskaya[2], P P Kuzhir[1,3], S A Maksimenko[1,3], E Flahaut[4], V Fierro[5], A Celzard[5] and G Valusis[2,6]

[1] Institute for Nuclear Problems, Belarus State University, Bobruiskaya 11, 220030 Minsk, Belarus
[2] Center for Physical Sciences and Technology, Sauletekio st. 3, Vilnius LT-10222, Lithuania
[3] Tomsk State University, 36, Lenin Avenue, Tomsk, 634050, Russia
[4] CIRIMAT, UMR CNRS 5085, 31062 Toulouse Cedex 9, France
[5] IJL, UMR Universite de Lorraine-CNRS 7198, ENSTIB, 27 Rue Philippe Seguin, CS 60036, 88026 Epinal Cedex, France
[6] Faculty of Physics, Vilnius University, Sauletekio 9/3, Vilnius LT-10222, Lithuania

E-mail: mikhail.shuba@gmail.com

Abstract

Due to the high polarizability of finite-length carbon nanotubes (CNTs) in the quasi-static regime, they can be considered as building blocks for the fabrication of high dielectric constant material. Our theoretical estimations, based on an effective medium approach and solutions of a boundary value problem for individual CNT, predict that composite materials comprising short-length CNTs can have very high dielectric constants (up to 300) and low dielectric loss tangents (below 0.03) in the terahertz range. In order to prove this, 500–1000 nm thick films comprising single- and multi-walled CNTs of both long (0.5–2 μm) and short (0.1–0.4 μm) lengths have been fabricated. The analysis, based on the time-domain terahertz spectroscopy in the range 0.2–1.0 THz, demonstrated a decrease in the dielectric loss tangents of the CNT-based materials with a reduction in CNT length. In the terahertz range, the films comprising short-length CNTs had a relative effective permittivity with a large real part (25–136) and dielectric loss tangent (0.35–0.60).

Keywords: thin film, effective permittivity, carbon nanotube, terahertz frequency range

[7] Author to whom correspondence should be addressed.

1. Introduction

Electromagnetic parameters of individual carbon nanotubes (CNTs) have been intensively studied over the past two decades [1–7]. It has been shown that strongly slowed down surface waves can propagate along metallic single-walled CNTs (SWCNT) [1], SWCNT bundles [3], and multi-walled CNTs (MWCNTs) [4]. Standing surface waves occur in finite-length SWCNTs at $\lambda_s \approx 2L$ [5, 6], where L is the nanotube length, and λ_s is wavelength of the surface wave. Resonant excitation of these waves by incident plane waves results in a length-dependent antenna resonance in the polarizability spectra of CNTs [6]; this is also called localized plasmon resonance (LPR) [8]. LPR causes experimentally observed terahertz conductivity peaks in MWCNT- and SWCNT-based composite media [9–11].

As discussed in [7], there are three regimes in which CNT interact with electromagnetic fields: quasi-static (at frequency range $f \ll f_s$, f_s being the frequency of the first antenna resonance), intermediate (or resonant, $f \approx f_s$), and dynamic ($f > f_s$). In the dynamic regime, the finite-length effect is negligibly small, the CNT absorption cross-section is proportional to the tube conductivity, and the imaginary part of the tube polarizability exceeds its real part. In the quasi-static regime, the real part of the carbon nanotube polarizability is practically the same as that at zero frequency, and energy dissipation is strongly suppressed by the screening effect. The latter is caused by a depolarizing field that almost compensates the axial component of the incident field [7].

For short-length ($L \approx 250$ nm) and long-length ($L \approx 1$ μm) SWCNTs, the terahertz resonances are expected at $f_s \approx 12$ THz and $f_s \approx 3$ THz, respectively [10]. This means that the quasi-static regime for short length tubes includes the terahertz range, $f < 2$ THz.

In the present study we report for the first time an observation of the quasi-static regime in the terahertz range for both short-length single- and multi-walled CNTs. Our investigation includes fabrication, measurement and analysis of the terahertz effective permittivity of thin films comprising both long ($L \geqslant 0.5$ μm) and short ($L \leqslant 0.3$ μm) CNTs.

Previously, the alternating-current conductivity and the effective permittivity of CNT films in the terahertz range have mainly only been studied experimentally [12–17]. The real part of the relative permittivity $\mathrm{Re}(\varepsilon_{\mathrm{eff}})$ and the dielectric loss tangent $\tan\delta = \mathrm{Im}(\varepsilon_{\mathrm{eff}})/\mathrm{Re}(\varepsilon_{\mathrm{eff}})$ of SWCNT films have been evaluated to be in the ranges 10–10^4 and 1–5, respectively [12, 13, 18]. A high value of $\tan\delta$ can be explained by two factors: (i) the use of long-length tubes (>0.5 μm) for film preparation; (ii) electrical contact between tubes resulting in the formation of a conductive network and partial suppression of the finite-length effect.

The fabrication of high constant dielectric terahertz materials is a real and important task. They concentrate the energy of terahertz frequency light into a small volume, thus enabling a reduction in the size of passive elements for terahertz optics. Moreover, these materials may be useful in the production of high-contrast periodic materials (or metamaterials) in the terahertz range. For these purposes, media with $\mathrm{Re}(\varepsilon_{\mathrm{eff}})$ maximized and $\tan\delta$ minimized are needed. Our investigation aims at demonstrating the potential for application of short-length CNTs as building blocks for high dielectric constant terahertz materials.

2. Theoretical consideration

In this section, we will theoretically consider a CNT-based composite material, where a high density of nanotubes are dispersed homogeneously throughout the material, and where each tube is electrically isolated from others. In this case, the electromagnetic parameters of the composite material will be primarily determined by the properties of the individual tubes.

Following the work of Slepyan [8], we used the adopted Waterman–Truell formula to estimate the relative effective permittivity of composite material containing CNT inclusions:

$$\varepsilon_{\mathrm{eff}}(\omega) = \varepsilon_h(\omega) + \frac{1}{3\varepsilon_0}\sum_j \int_0^\infty \alpha_j(\omega, L) N_j(L)\mathrm{d}L, \qquad (1)$$

where ε_h is the relative permittivity of the host material; $\varepsilon_0 = 8.85 \times 10^{-12}$ F m^{-1}; the function $N_j(L)$ describes the number density of the inclusions of type j with radius R_j and length L; the factor 1/3 in (1) is due to the random orientations of the CNTs; and α_j is the axial polarizability of inclusion, calculated using the integral equation technique described in [6], [19] and [7] for SWCNT, SWCNT bundle and MWCNT, respectively. Equation (1) ignores the electromagnetic interactions between inclusions in the composites, i.e. it is valid when all the inclusions can be considered to be electrically isolated from each other.

In our calculations we used $\varepsilon_h = 1$ and the volume fraction occupied together by the inclusions was $F = 20\%$. For simplicity, each composite material considered contained identical inclusions. To calculate the axial conductivity of the metallic SWCNTs, the doped semiconducting SWCNTs, and the metallic shells of the MWCNTs, we used the Drude formula [1] with an electron relaxation time of 40 fs for the SWCNTs [8] and 10 fs for the MWCNTs [20].

Figure 1 shows the calculated frequency dependence of the real part of the relative effective permittivity $\mathrm{Re}(\varepsilon_{\mathrm{eff}})$ and the dielectric loss tangent $\tan\delta$ of composites with different, but consistent within each sample, nanotube lengths. Let us note that figure 1 shows the relative effective permittivity in the frequency range below the LPR of the SWCNT, and the lines are discontinuous at the LPR. Due to the finite length effect [6], an individual, isolated SWCNT has a polarizability with a large real part $\mathrm{Re}(\alpha)$ and a small imaginary part $\mathrm{Im}(\alpha)$ in the quasi-static regime. This regime occurs up to 1 THz for $L = 400$ nm and 10 THz for $L = 100$ nm.

As one can see in figure 1, in the terahertz range, SWCNT-based composite materials behave like a high-dielectric constant material. In particular, for composites containing CNTs with a tube length of $L = 400$ nm, $\mathrm{Re}(\varepsilon_{\mathrm{eff}}) \approx 1000$ and $\tan\delta < 0.1$ at $f < 1$ THz. For composites containing CNTs with a tube length of $L = 200$ nm, $\mathrm{Re}(\varepsilon_{\mathrm{eff}}) \approx 320$ and $\tan\delta < 0.1$ at $f < 3.5$ THz. Finally, for composites containing CNTs with a tube length of $L = 100$ nm, $\mathrm{Re}(\varepsilon_{\mathrm{eff}}) \approx 90$ and $\tan\delta < 0.1$ at $f < 10$ THz.

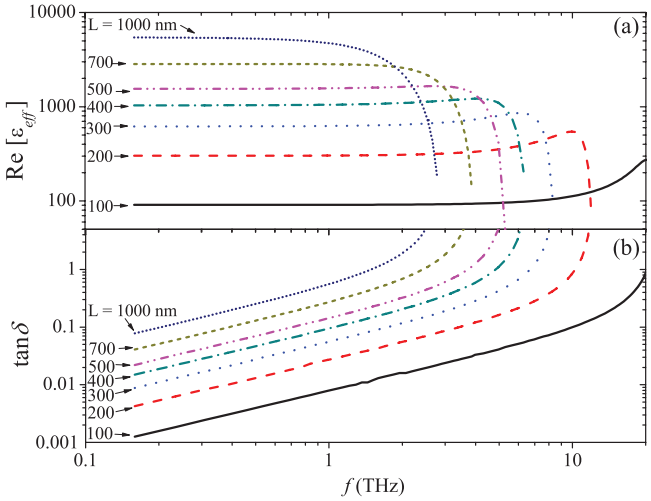

Figure 1. Frequency dependence of (a) $\mathrm{Re}(\varepsilon_{\mathrm{eff}})$ and (b) $\tan\delta$ for a composite comprising metallic zigzag (12, 0) individual SWCNTs with nanotube lengths $L \in \{100, 200, 300, 400, 500, 700, 1000\}$ nm.

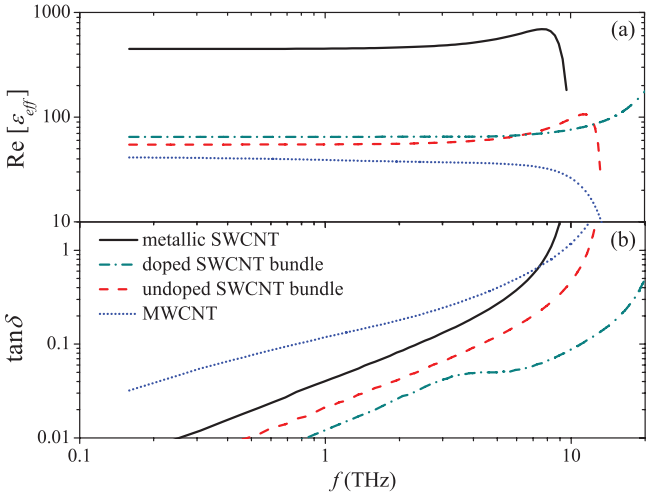

Figure 2. Frequency dependence of (a) $\mathrm{Re}(\varepsilon_{\mathrm{eff}})$ and (b) $\tan\delta$ for composites comprising identical individual (12, 0) metallic SWCNTs, undoped or doped SWCNT bundles, and MWCNTs. Each bundle has a diameter of 3.5 nm and comprises five semiconducting tubes with indexes (13, 0) and two metallic tubes with indexes (12, 0). The conductivity of the semiconducting tubes in the doped bundle should be the same as for the metallic SWCNTs. The MWCNTs have an outer diameter of 4.6 nm and comprise 9 shells with chiral indexes $(8p + 12, 0)$, $p \in \{0, 1, 2, ..., 8\}$. Consequently, they possess two consecutive semiconducting shells, which are followed by a metallic shell. Each inclusion has length of 250 nm.

Figure 2 shows the frequency dependence of $\mathrm{Re}(\varepsilon_{\mathrm{eff}})$ and $\tan\delta$ for composites comprising identical metallic SWCNTs, undoped and doped bundles of SWCNTs, and individual MWCNTs at the same length and volume fraction of the inclusions. After comparing the parameters of composites containing different CNT inclusions, we can conclude that the individual SWCNTs are the most appropriate for producing high dielectric contrast materials in the terahertz range. All the considered CNT inclusions have approximately the same polarizability; however, the number density of SWCNTs is much higher than that of other types of CNTs. This explains one advantage SWCNTs have over other types of tubes.

The parameters of the composite comprising MWCNTs of different diameters are described theoretically in [7]. Let us note that since the number density of MWCNTs in the film is higher for thinner tubes, and MWCNT polarizability slightly depends on the number of walls in the quasi-static regime [7], a higher terahertz permittivity is expected for the films comprising thinner MWCNTs.

As shown in figure 2(b), for composites comprising doped and undoped bundles of SWCNTs, doping leads to an increase of $\mathrm{Re}(\varepsilon_{\mathrm{eff}})$ and to a decrease of $\tan\delta$. The LPR frequency is higher for doped bundles [3] resulting in the observed lower energy dissipation in doped bundles than in undoped ones. As the electron relaxation time is shorter for MWCNTs than for bundle of SWCNTs, the value of $\tan\delta$ is lower for SWCNT bundle than for MWCNT-based composite (see figure 2(b)).

Let us note that the fabrication of composites with non-percolating tubes with high tube volume fraction is a non-trivial task, as SWCNTs tend to aggregate even at $F = 1\%$ due to electrostatic interaction. Meanwhile, the tendency to the high $\mathrm{Re}(\varepsilon_{\mathrm{eff}})$ and low $\tan\delta$ predicted in figures 1 and 2 occurs even in the network of short-length CNTs. In section 3 we will experimentally show that SWCNT-based films comprising short length CNTs (with $L < 300$ nm) behave like high dielectric constant materials in the terahertz range, i.e. they have $\mathrm{Re}(\varepsilon_{\mathrm{eff}}) \geqslant 100$ and $\tan\delta \leqslant 0.5$.

Table 1. Details of the samples prepared: D, L_m and Δ are diameter, mean and standard deviation of the length of the SWCNT bundles and the individual MWCNTs, respectively. $I_{\mathrm{D}}/I_{\mathrm{G}}$ is the ratio of the integrated area of the D-band to that of the G-band in Raman spectra at an excitation wavelengths of 532 nm.

Sample type	L_m (μm)	Δ (μm)	D (nm)	$I_{\mathrm{D}}/I_{\mathrm{G}}$
Long SWCNTs	0.80	0.40	1–5	0.17
Short SWCNTs	0.20	0.12	1–3	0.28
Long MWCNTs	0.50	0.21	8–20	1.30
Short MWCNTs	0.19	0.08	8–20	1.30

3. Experimental results and discussion

In our experiment we used different CNT materials: (i) purified SWCNTs (Nanointegris Technology Inc., Batch PO568) produced by gas-phase catalysis (HiPCO process) with an average diameter of 1 nm, and a purity exceeding 95%; and (ii) MWCNTs produced by CVD (Bayer Baytubes) with a length of <1 μm, an inner diameter of $\sim$4 nm and an outer diameter of $\sim$13 nm. We also did experiments with double-walled CNTs; all the data concerning this material are presented in supplementary data (stacks.iop.org/JPhysD/50/08LT01/mmedia)[8]. Short-length CNTs (50–300 nm) were prepared using a soft cutting approach developed in [21].

CNT films were fabricated via the vacuum filtration technique [22]. The film thicknesses d, measured with the profilometer Veeco Dektak 6M, were in the range of 300–1000 nm. In order to

[8] See supplementory data for details of the CNT cutting method, CNT film preparation and characterisation, as well as the experimental data for double-walled CNT films.

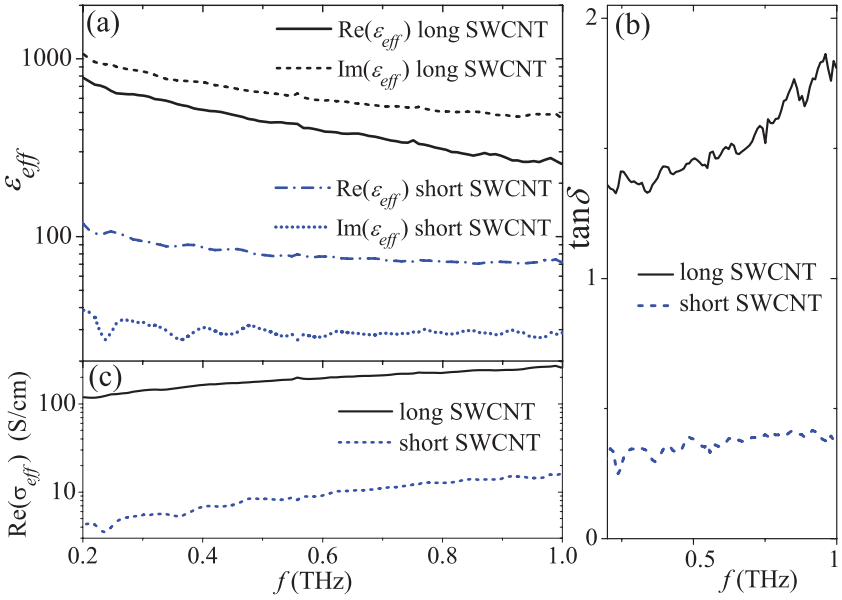

Figure 3. Frequency dependence of (a) Re(ε_{eff}) and Im(ε_{eff}), (b) tan δ, and (c) Re(σ_{eff}) for SWCNT samples comprising short and long carbon nanotubes.

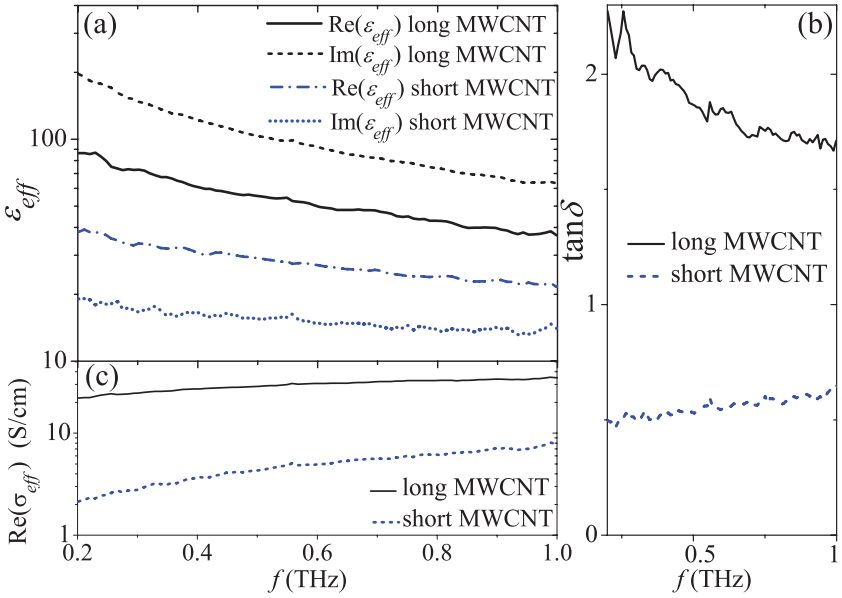

Figure 4. Same as figure 3, but for a MWCNT film.

dope SWCNT thin films, droplets of 1 M HNO_3 were placed on samples and allowed to dry for 12 h. This process leads to p-type doping of SWCNTs [23]. Details of the sample preparation and characterization are presented in supplementary data[9].

The length and diameter of SWCNT bundles and individual MWCNTs, obtained using atomic force microscopy (AFM, Solver P47 PRO, NT-MDT, Inc.), are collected in table 1. One can see from table 1 that the applied cutting strategy effectively reduced the CNT lengths. Cutting also led to partial debundling of the SWCNTs: i.e. the maximal bundle diameter was reduced after cutting.

[9] See footnote 8.

Table 2. Real part of the relative effective permittivity Re(ε_{eff}), dielectric loss tangent tan δ, and real part of the effective conductivity Re(σ_{eff}) for CNT films comprising short and long carbon nanotubes at 0.75 THz.

Sample type	Re(ε_{eff})	tan δ	Re(σ_{eff}) (S cm^{-1})
Long SWCNTs	360	1.6	200
Doped long SWCNTs	660	2	500
Short SWCNTs	73	0.4	12
Doped short SWCNTs	136	0.35	19
Long MWCNTs	48	1.7	32
Short MWCNTs	25	0.6	5

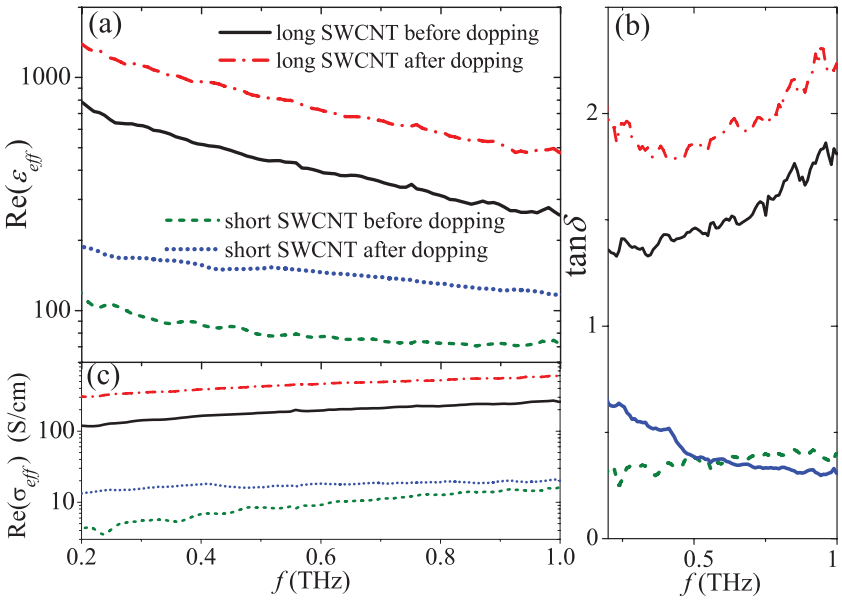

Figure 5. Frequency dependence of (a) $\mathrm{Re}(\varepsilon_{\mathrm{eff}})$, (b) $\tan\delta$, and (c) $\mathrm{Re}(\sigma_{\mathrm{eff}})$ for samples comprising SWCNTs, both before and after doping.

Raman spectroscopy was used to estimate the crystalline quality of the CNTs. Measurements were performed using the Raman spectrometer combined with the confocal microscope Nanofinder High End (Tokyo Instruments) with 532 nm wavelength laser excitation. A ratio of the integrated area of the D-band (1300–1350 cm^{-1}) to that of the G-band (1520–1600 cm^{-1}) $I_{\mathrm{D}}/I_{\mathrm{G}}$ was taken as a measure of the CNT crystalline quality [21]: the lower the value of $I_{\mathrm{D}}/I_{\mathrm{G}}$, the lower the concentration of sidewall defects in the CNTs. The value $I_{\mathrm{D}}/I_{\mathrm{G}}$ is presented in table 1 for short- and long-length CNTs. Small changes in the ratio $I_{\mathrm{D}}/I_{\mathrm{G}}$ indicate that cutting slightly disturbs the crystalline structure of the CNTs.

The measurements of the complex transmission were conducted under normal incidence in the frequency range $f \in (0.2, 1)$ THz by means of time-domain terahertz spectrometry (EKSPLA, Vilnius Lithunia) with a femtosecond laser (wavelength 1 μm, with a pulse duration of less than 150 fs) and a GaBiAs photoconductive switch. Typical terahertz pulses with and without the samples, as well as the transmission spectra are shown in supplementary data[10]. Spectra of the effective permittivity of the CNT films were calculated using the Fourier transform of the measured time-domain signal.

Figures 3 and 4 show the frequency dependencies of $\mathrm{Re}(\varepsilon_{\mathrm{eff}})$, $\mathrm{Im}(\varepsilon_{\mathrm{eff}})$, $\tan\delta$, and the real part of the effective conductivity, $\mathrm{Re}(\sigma_{\mathrm{eff}}) = \varepsilon_0\omega\mathrm{Im}(\varepsilon_{\mathrm{eff}})$, of the samples comprising short and long SWCNTs and MWCNTs. As shown in figures 3 and 4, all the values of $\mathrm{Re}(\varepsilon_{\mathrm{eff}})$, $\mathrm{Im}(\varepsilon_{\mathrm{eff}})$, $\tan\delta$, and $\mathrm{Re}(\sigma_{\mathrm{eff}})$ decrease drastically as the average length of the tubes decreases by about three times (from 0.5–1 μm to 100–300 nm).

In order to quantitatively compare the parameters of the different types of CNT films, the values $\mathrm{Re}(\varepsilon_{\mathrm{eff}})$, $\tan\delta$, and $\mathrm{Re}(\sigma_{\mathrm{eff}})$ for different samples at 0.75 THz are given in table 2. One can see from table 2 that, for SWCNT and MWCNT samples respectively, cutting leads to a reduction in the value of $\mathrm{Re}(\sigma_{\mathrm{eff}})$ by about 17 and 6 times and in the value $\mathrm{Re}(\varepsilon_{\mathrm{eff}})$ by about 5 and 1.9 times. As a result, the loss tangent decreases by 4 and 2.8 times after cutting of SWCNTs and MWCNTs, respectively.

Simultaneously with quantitative variations of the terahertz parameters we observed their qualitative changes. Resonance and dynamic regime of long-length CNT interaction with the terahertz field [7] leads to high energy dissipation in the CNTs. Long-length CNT samples could be associated with metallic films for which the value of $\mathrm{Re}(\sigma_{\mathrm{eff}})$ is high and $\tan\delta \gg 1$. Quasi-static regime of short-length CNT interaction with terahertz radiation causes small energy dissipation preserving high value of the real part of the CNT polarizability. The parameters of short-length CNT samples are close to that of high dielectric constant terahertz materials with high $\mathrm{Re}(\varepsilon_{\mathrm{eff}})$ and $\tan\delta \ll 1$. As follows from table 2, out of all CNT types, the SWCNTs are the most perspective nanoparticles for fabrication of high dielectric constant material for the terahertz range. Thin film comprising short SWCNTs demonstrates $\mathrm{Re}(\varepsilon_{\mathrm{eff}}) = 73$ and $\tan\delta = 0.4$ at 0.75 THz. We believe that loss tangent could be reduced if the SWCNTs were electrically isolated from each other in the film.

Figure 5 shows the frequency dependence of $\mathrm{Re}(\varepsilon_{\mathrm{eff}})$, $\tan\delta$, and $\mathrm{Re}(\sigma_{\mathrm{eff}})$ for SWCNT films before and after the doping by nitric acid. Acid complexes attached to the tube walls cause p-type doping effects [23] which leads to the 'metallization' of the semiconducting SWCNTs and a blue shift of the LPR in SWCNT bundles [19]. As shown in figures 5(a) and (c), doping leads to an increase of both $\mathrm{Re}(\varepsilon_{\mathrm{eff}})$ and $\mathrm{Re}(\sigma_{\mathrm{eff}})$. Since doping reduces intertube contact conductance, the depolarizing field diminishes and terahertz energy dissipation in SWCNTs increases. This explains the increase in the loss tangent $\tan\delta$ at lower frequencies (<0.5 THz) after doping (see figure 5(b)). Comparison of the terahertz parameters given in table 2 for SWCNT films before and after doping demonstrates a doubling of the value of $\mathrm{Re}(\varepsilon_{\mathrm{eff}})$ and a slight reduction of $\tan\delta$ at 0.75 THz due to the doping process. So, for doped SWCNT film, we obtained $\mathrm{Re}(\varepsilon_{\mathrm{eff}}) = 136$ and $\tan\delta = 0.35$ at 0.75 THz.

[10] See footnote 8.

This is very promising for the application of short-length SWCNTs as building blocks for high dielectric constant material in the terahertz range. Let us note that the real part of the relative permittivity of known low loss dielectric materials in the terahertz range generally does not exceed 100 [24].

The frequency dependency of the value $\mathrm{Re}(\sigma_{\mathrm{eff}})$ in figures 3–5(c) do not follow the Drude law for all the CNT samples (we observed $\partial \mathrm{Re}(\sigma_{\mathrm{eff}})/\partial\omega > 0$, which is the opposite of that predicted by the Drude law). Moreover, the frequency dependence of $\mathrm{Re}(\sigma_{\mathrm{eff}})$ is stronger for short tubes than for long ones. Non-Drude-like behavior appears due to the LPR at higher frequencies (>1 THz), caused by the finite-length of the tubes in the SWCNT samples. The shorter the tube length, the higher the LPR frequency, and the stronger the finite-length effect in the considered frequency range. As was observed in experiments [10], LPR occurs at about 6 and 30 THz for long ($\approx$1 μm) and short ($\approx$0.2 μm) SWCNT bundles, respectively. The LPR in short-length MWCNTs is expected to lie in the range $f \in (10, 40)$ THz, however it is suppressed by interband electron transitions at the large shell diameters (>5 nm) [4]. The LPR in long MWCNTs (>1 μm) has been observed in [11] and theoretically described in [7].

As there is no theoretical model tacking into account CNT coupling, and as CNT-based media are quite complex (there is a distribution over length and diameter of CNT bundles), we cannot describe theoretically our experimental data. Meanwhile, we have shown that the tendency to the high $\mathrm{Re}(\sigma_{\mathrm{eff}})$ and low $\tan\delta$ (predicted for composite of electrically isolated CNTs) occurs even in the network of electrically coupled short-length CNTs. Probably, this is due to the quite high intertube contact resistance, which results in the low coupling of adjacent tubes in our samples.

4. Conclusions

The effective medium theory has been applied to explain the relative effective permittivity of composite material comprising electrically isolated CNTs. Comparative analysis has been done for composites containing individual SWCNTs, doped and undoped SWCNT bundles, and MWCNTs at a high (20%) volume fraction. It has been found that among different modifications of CNTs, individual short-length SWCNTs ($L < 400$ nm) are the most promising inclusions for fabrication of high dielectric constant material in the terahertz range.

Thin films comprising (i) doped and undoped SWCNT bundles, and (ii) individual MWCNTs of different lengths (about 1 and 0.2 μm) have been fabricated and studied by terahertz time-domain spectroscopy over the frequency range from 0.2 to 1 THz. It has been shown that a reduction in the CNT length leads to a decrease in the dielectric loss tangent of the films, while preserving a high value of the real part of the relative effective permittivity. Experimental data proved that the quasi-electrostatic regime occurs in the terahertz range for all the short-length CNTs considered. Fabricated film comprising bundles of doped SWCNTs, each with a length of about 200 nm, has $\mathrm{Re}(\varepsilon_{\mathrm{eff}}) = 136$ and $\tan\delta = 0.35$ at 0.75 THz. The value $\mathrm{Re}(\varepsilon_{\mathrm{eff}})$ can be increased if one uses individual tubes instead of bundled ones. Alignment of the tubes will lead to an increase in the component of the permittivity tensor in the direction of the tube axis. This will enable the fabrication of high relative dielectric constant anisotropic terahertz materials.

Acknowledgments

This research was funded by Ministry of Education and Science of Russian Federation, project ID RFMEFI57714X0006.

References

[1] Slepyan G Y, Maksimenko S A, Lakhtakia A, Yevtushenko O and Gusakov A V 1999 *Phys. Rev.* B **60** 17136–49
[2] Hartmann R R, Kono J and Portnoi M E 2014 *Nanotechnology* **25** 322001
[3] Shuba M V, Maksimenko S A and Lakhtakia A 2007 *Phys. Rev.* B **76** 155407
[4] Shuba M V, Slepyan G Y, Maksimenko S A, Thomsen C and Lakhtakia A 2009 *Phys. Rev.* B **79** 155403
[5] Hanson G 2005 *IEEE Trans. Antennas Propag.* **53** 3426–35
[6] Slepyan G Y, Shuba M V, Maksimenko S A and Lakhtakia A 2006 *Phys. Rev.* B **73** 195416
[7] Shuba M V, Melnikov A V, Paddubskaya A G, Kuzhir P P, Maksimenko S A and Thomsen C 2013 *Phys. Rev.* B **88** 045436
[8] Slepyan G Y, Shuba M V, Maksimenko S A, Thomsen C and Lakhtakia A 2010 *Phys. Rev.* B **81** 205423
[9] Ugawa A, Hwang J, Gommans H, Tashiro H, Rinzler A and Tanner D 2001 *Curr. Appl. Phys.* **1** 45–9
[10] Shuba M V *et al* 2012 *Phys. Rev.* B **85** 165435
[11] Morimoto T and Okazaki T 2015 *Appl. Phys. Express* **8** 055101
[12] Jeon T I, Kim K J, Kang C, Maeng I H, Son J H, An K H, Lee J Y and Lee Y H 2004 *J. Appl. Phys.* **95** 5736–40
[13] Seo M A, Yim J H, Ahn Y H, Rotermund F, Kim D S, Lee S and Lim H 2008 *Appl. Phys. Lett.* **93** 231905
[14] Wang L, Zhou R and Xin H 2008 *IEEE Trans. Microw. Theory Tech.* **56** 499–506
[15] Maine S, Koechlin C, Rennesson S, Jaeck J, Salort S, Chassagne B, Pardo F, Pelouard J L and Haïdar R 2012 *Appl. Opt.* **51** 3031–5
[16] Chimowa G, Flahaut E and Bhattacharyya S 2014 *Appl. Phys. Lett.* **105** 173511
[17] Zhang Q, Haroz E H, Jin Z, Ren L, Wang X, Arvidson R S, Luttge A and Kono J 2013 *Nano Lett.* **13** 5991–6
[18] Dadrasnia E, Puthukodan S and Lamela H 2014 *J. Nanophotonics* **8** 083099
[19] Nemilentsau A M, Shuba M V, Slepyan G Y, Kuzhir P P, Maksimenko S A, D'yachkov P N and Lakhtakia A 2010 *Phys. Rev.* B **82** 235424
[20] Chiu H Y, Deshpande V V, Postma H W C, Lau C N, Mikó C, Forró L and Bockrath M 2005 *Phys. Rev. Lett.* **95** 226101
[21] Shuba M V, Paddubskaya A G, Kuzhir P P, Maksimenko S A, Ksenevich V K, Niaura G, Seliuta D, Kasalynas I and Valusis G 2012 *Nanotechnology* **23** 495714
[22] Hennrich F, Lebedkin S, Malik S, Tracy J, Barczewski M, Rosner H and Kappes M 2002 *Phys. Chem. Chem. Phys.* **4** 2273–7
[23] Hennrich F, Wellmann R, Malik S, Lebedkin S and Kappes M M 2003 *Phys. Chem. Chem. Phys.* **5** 178–83
[24] Bolivar P H, Brucherseifer M, Rivas J G, Gonzalo R, Ederra I, Reynolds A L, Holker M and de Maagt P 2003 *IEEE Trans. Microw. Theory Tech.* **51** 1062–6